

Energy-dependent rotational polarization in elementary rearrangement collisions

Nark Nyul Choi

Department of Physics, Kumoh National University of Technology, Kumi, Kyungbook 730-701, Korea

Sung-Ho Suck Salk

Department of Physics, Pohang University of Science and Technology, Pohang, Kyungbook 790-874, Korea

(Received 6 March 1995)

A rigorous method of describing the energy dependence of rotational polarization in rearrangement collisions is proposed by exploring both the kernel function of intrinsic nature and the distorted-wave functions of dynamic nature. From this study the energy dependence of rotational polarization and favored geometric configuration is well understood in an explicit manner. It is also found that the rotational polarization is not affected by the interference of partial waves.

PACS number(s): 34.50.Lf, 34.50.Pi, 34.90.+q

We propose a rigorous approach for explaining the energy dependence of rotational polarization in rearrangement collisions by introducing a combined examination of both the kernel function and the distorted-wave functions. Based on this approach, the energy dependence of rotational polarization is well understood for elementary atom-diatom molecule reaction processes. Further, a recently introduced pseudokernel function is found to be a highly useful tool for revealing a favored geometric configuration in elementary rearrangement collision processes.

To the best of our knowledge, there exists no simple theory to reveal physical mechanisms of elementary reaction processes without excessive computation. It is thus of great demand to devise a method which is simple to use in order to extract useful information on a reaction mechanism. Our objective here is to propose such a simple method of studying the energy dependence of rotational polarization, by utilizing the space-fixed representation in our distorted-wave Born approximation (DWBA) theory [1,2]. It has a unique merit of separating the T matrix into a static factor (the kernel function) and a dynamic factor (the distorted-wave functions). Preferential rotational polarization in atom-diatom mol-

ecule rearrangement collision processes depends on both collision energy and interaction potential. According to our DWBA theory, information on dynamics is obtained from the distorted-wave functions, which depend on the former, and intrinsic or static property is extracted from the kernel function, which depends on the latter.

Despite its failure in the prediction of absolute magnitudes for integrated cross sections, at low collision energies the single-channel DWBA has proven to be accurate in reproducing the relative (but not absolute) magnitudes of the integrated cross sections, the structure of the angular distributions [3], and the product rotational-vibrational distributions [4–8]. The DWBA is a useful tool for qualitative understanding, but not for quantitative accuracy. In order to examine the energy dependence of favored rotational polarization, we propose a rigorous approach by introducing a combined examination of both the distorted-wave function and the kernel distribution function. Based on our earlier DWBA formalism [1], a reduced form of the integral cross section for the state-to-state reactive scattering (rearrangement collision) $A + BC(n_a, j_a, m_a) \rightarrow AB(n_b, j_b, m_b) + C$ can be cast into

$$\begin{aligned} \sigma(n_a j_a m_a \rightarrow n_b j_b m_b) &= J^2 \frac{\mu_a \mu_b}{(2\pi)^2} \frac{K_b}{K_a} \int d\hat{\mathbf{K}}_b \left| \int d\mathbf{R}_b d\mathbf{R}_a \chi_b^{(-)*}(\mathbf{K}_b, \mathbf{R}_b) r_b^{j_b} Y_{j_b m_b}^*(\hat{\mathbf{r}}_b) g(R_b, R_a, \hat{\mathbf{R}}_b \cdot \hat{\mathbf{R}}_a) r_a^{j_a} Y_{j_a m_a}(\hat{\mathbf{r}}_a) \chi_a^{(+)}(\mathbf{K}_a, \mathbf{R}_a) \right|^2, \end{aligned} \quad (1)$$

where $g(R_b, R_a, \hat{\mathbf{R}}_b \cdot \hat{\mathbf{R}}_a)$ is defined as

$$g(R_b, R_a, \hat{\mathbf{R}}_b \cdot \hat{\mathbf{R}}_a) = \frac{u_{j_b}(r_b)}{r_b^{j_b+1}} W(R_b, R_a, \hat{\mathbf{R}}_b \cdot \hat{\mathbf{R}}_a) \frac{u_{j_a}(r_a)}{r_a^{j_a+1}}. \quad (2)$$

Here n_a (n_b), j_a (j_b), and m_a (m_b) are, respectively, the vibrational, rotational, and polarizational quantum numbers of the reactant (product) molecule. J is the Jacobian of the

coordinate transformation from the internal to external coordinates. The definitions of coordinate vectors are shown in Fig. 1. μ_a (μ_b) and \mathbf{K}_a (\mathbf{K}_b) are, respectively, the reduced mass and the wave vector for the reactant (product) channel. $\chi_a^{(+)}(\mathbf{K}_a, \mathbf{R}_a)$ and $\chi_b^{(-)}(\mathbf{K}_b, \mathbf{R}_b)$ are the outgoing and ingoing single-channel distorted-wave functions, respectively, for the reactant and product channels. $u_{j_a}(r_a)$ and $u_{j_b}(r_b)$ are separately the reactant and product molecular radial wave functions. The newly defined kernel function in (2) differs

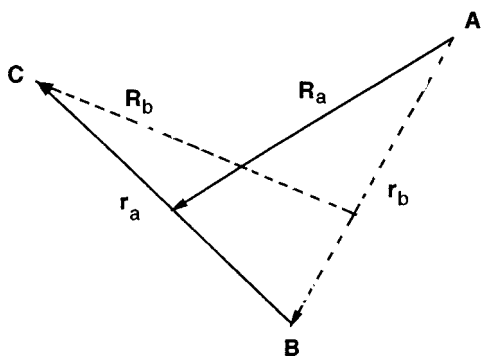
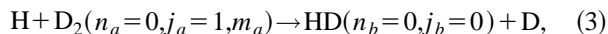


FIG. 1. Vector diagram of reactive scattering $A + BC \rightarrow AB + C$. The continuous line is for the reactant channel configuration while the dashed line is for the product channel configuration.

from the earlier one [1] in that it now has an advantage of allowing the study of angular dependence between \mathbf{R}_a and \mathbf{R}_b or, equivalently, between \mathbf{r}_a and \mathbf{R}_a . Finally, $W(R_b, R_a, \hat{\mathbf{R}}_b \cdot \hat{\mathbf{R}}_a)$ is the perturbation potential responsible for opening a product arrangement channel.

The state-to-state reactive transition of present interest is



with $m_a=0$ and 1. The potential-energy surface (PES) used in this study is the LSTH (Liu-Siegbahn-Truhlar-Horowitz PES) which is the same as that used in Ref. [9]. The computation of the distorting potential and the distorted-wave functions are based on our earlier method [1–3, 6–10]. For simplicity, we select the rotational states of $j_a=1$ and $j_b=0$. Hereafter we denote $\sigma(01m_a \rightarrow 000)$ as $\sigma(m_a)$ for brevity.

The present space-fixed DWBA method has a clear merit of separating the transition amplitude in the energy-independent static part, i.e., the kernel distribution function, and the energy-dependent dynamic part, i.e., the distorted-wave functions. In the present study we take full advantage of this merit. Information on the favored geometry of the triatomic system can be obtained from the angular structure of the kernel $g(R_b, R_a, \hat{\mathbf{R}}_b \cdot \hat{\mathbf{R}}_a)$ or equivalently $g(r_a, R_a, \hat{\mathbf{r}}_a \cdot \hat{\mathbf{R}}_a)$. On the other hand, the product of the distorted-wave functions $\chi_a^{(+)}(\mathbf{K}_a, \mathbf{R}_a)$ and $\chi_b^{(-)}(\mathbf{K}_b, \mathbf{R}_b)$ in (1) directly yields information on the dynamics of rearrangement collision processes which, in turn, affects polarization.

We first examine the variation of the ratio $\sigma(1)/\sigma(0)$ with collision energy E_K . As shown in Fig. 2, the lower the collision energy, the smaller the ratio $\sigma(1)/\sigma(0)$, thus indicating that $m_a=0$ is a preferred rotational polarization. Encouragingly this qualitative prediction is in perfect agreement with the exact close-coupling study of Schatz and Kupperman [9]. We find that the relative strength of $m_a=1$ polarization compared to $m_a=0$, that is, $\sigma(1)/\sigma(0)$, increases with collision energy, showing a strong nonlinearity in collision energy, as shown in Fig. 2. Importantly, we note that interference of reactive transition probability amplitudes does not affect the favored rotational polarization, showing the nature of incoherence. The rotational polarization is thus seen to be dynamic in nature as it depends on the incident collision energy. At low collision energies the favored rota-

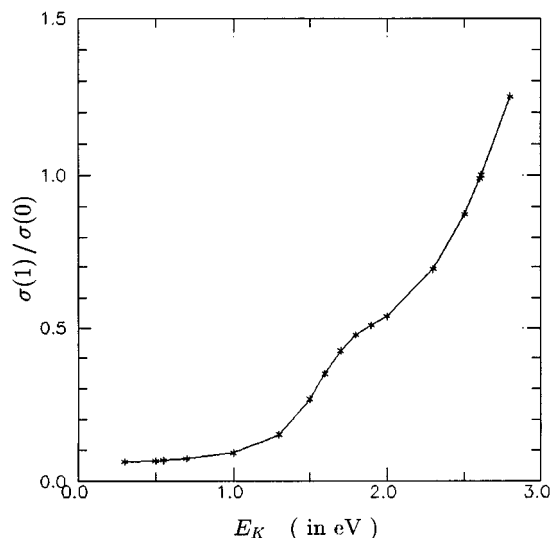


FIG. 2. The ratio of $\sigma(1)$ to $\sigma(0)$ for the reactive scattering $\text{H} + \text{D}_2(n_a=0, j_a=1) \rightarrow \text{HD}(n_b=0, j_b=0) + \text{D}$ as a function of collision energy.

tional polarization is readily understood from the structure of the kernel function alone, this indicating the importance of the static (or intrinsic) property of reactive systems. At higher collision energies, we find that the combined examination of both the kernel distribution and the distorted wave function is necessary.

In Fig. 3 we display the contour map of the distorted wave functions $|\chi^{(+)}(\mathbf{K}_a, \mathbf{R}_a)|$ at the incident collision energies of $E_K=0.55$ and 2.61 eV, respectively. The origin is chosen to be the center of mass of D_2 . The positive x axis is defined by $R_{\parallel} \equiv -\mathbf{R}_a // \mathbf{K}_a$ and the positive y axis by $R_{\perp} \equiv -\mathbf{R}_a \perp \mathbf{K}_a$. Following Fig. 1, each point in the $(R_{\parallel}, R_{\perp})$ plane represents $-\mathbf{R}_a$, i.e., the location of the incident atom H with respect to the center of mass of the diatomic molecule D_2 . Its direction is defined by $\theta = \cos^{-1}(-\mathbf{R}_a \cdot \mathbf{K}_a)$, that is, the angle between \mathbf{K}_a and $-\mathbf{R}_a$. The contour values in Fig. 3 are meaningful only in the order of magnitude sense. The greatest contribution to the distorted-wave function is seen to come from the positive R_{\parallel} axis, judging from the density of contour lines in Fig. 3. That is, the projectile is more likely found in the backward direction during the moment of reactive transition. This is owing to the repulsive part of interaction between the projectile H atom and the target D_2 molecule.

In Fig. 4 we plot the kernel distribution as a function of interatomic displacement vector \mathbf{r}_a at two fixed reactant channel classical turning points: $R_a^0=3.0$ and 1.5 a.u., which correspond to the collision energies of $E_K=0.55$ and 2.61 eV, respectively. The contour values are labeled by the powers of 10. The positive x axis denoted as r_{\parallel} represents that \mathbf{r}_a is antiparallel with \mathbf{R}_a , and the y axis denoted as r_{\perp} stands for $\mathbf{r}_a \perp \mathbf{R}_a$, with $r_{\parallel}=0.5r_a$ and $r_{\perp}=0.5r_a$, respectively. Each point in the plane represents $0.5\mathbf{r}_a$, i.e., the displacement vector of the atom D with respect to the center of mass of D_2 for a fixed reactant channel radius vector \mathbf{R}_a [see inset in Fig. 4(a)]. The origin of the $(r_{\parallel}, r_{\perp})$ plane corresponds to the center of mass of D_2 . Points on the x axis represent collinear configurations of HD_2 . Departure from

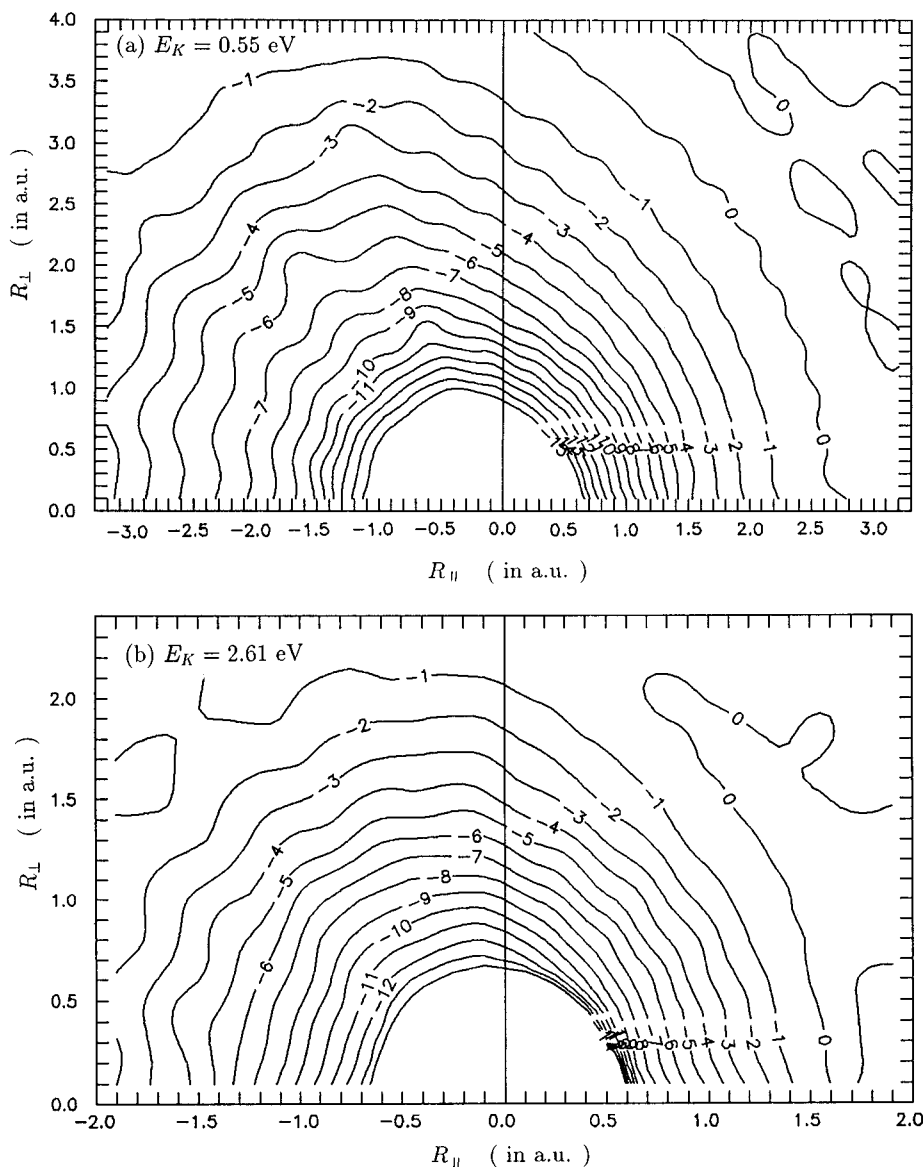


FIG. 3. Polar representations of contour maps of the reactant channel distorted-wave functions $|\chi_a^{(+)}(\mathbf{K}_a, \mathbf{R}_a)|$ at the collision energies of (a) 0.55 eV and (b) 2.61 eV for the reactive scattering $\text{H} + \text{D}_2(n_a=0, j_a=1) \rightarrow \text{HD}(n_b=0, j_b=0) + \text{D}$. The values are labeled by the powers of 10, e.g., -3 stands for 10^{-3} .

this x axis measures the degree of nonlinearity. We now find that the collinear configuration is dominant at a lower collision energy of 0.55 eV. This occurs where a trajectory (the solid circle) with $R_b = R_a$ crosses the r_{\parallel} axis, as seen from Fig. 4(a). As the collision energy increases, the angle made by \mathbf{R}_a and \mathbf{R}_b (or \mathbf{r}_a and \mathbf{R}_a) is seen to increase, suggesting departure from collinearity. This alters the best overlap region of the kernel distribution, which allows us to find the most favored transition-state geometry. The solid circles represent the trajectories of classical turning points; $R_b = R_a = 3.0$ and 1.5 a.u. Indeed, at a sufficiently high collision energy of 2.61 eV, the largest contribution of the kernel evaluated at the classical turning point is predicted to come from the area near a point denoted as x in Fig. 4(b). Thus the favored transition-state geometry is no longer collinear at high collision energies.

We are now ready to explicitly demonstrate that the com-

binational examination of both the distorted-wave functions and the kernel distribution function brings forth useful information on the energy dependence of rotational polarization. The kernel distribution, i.e., the static factor, is independent of collision energy whereas the distorted-wave functions, i.e., the dynamic factors, are energy dependent. Thus it is of great interest to see how the rotational polarization is affected by the interplay of the static and dynamic factors. The favored rotational polarization can be rigorously understood from the information of both the preferred orientation of \mathbf{R}_a relative to \mathbf{K}_a and the favored geometric configuration defined by an angle between \mathbf{R}_a and \mathbf{R}_b or \mathbf{r}_a and \mathbf{R}_a . To be specific, from the distorted-wave function $\chi_a^{(+)}$ we can determine the favored location \mathbf{R}_a of the incoming projectile atom. This, in turn, defines its best overlap region with the kernel distribution function.

There can be reactive scattering systems for which the angular structure of $\chi_a^{(+)}$ shows no backward peak. In such a

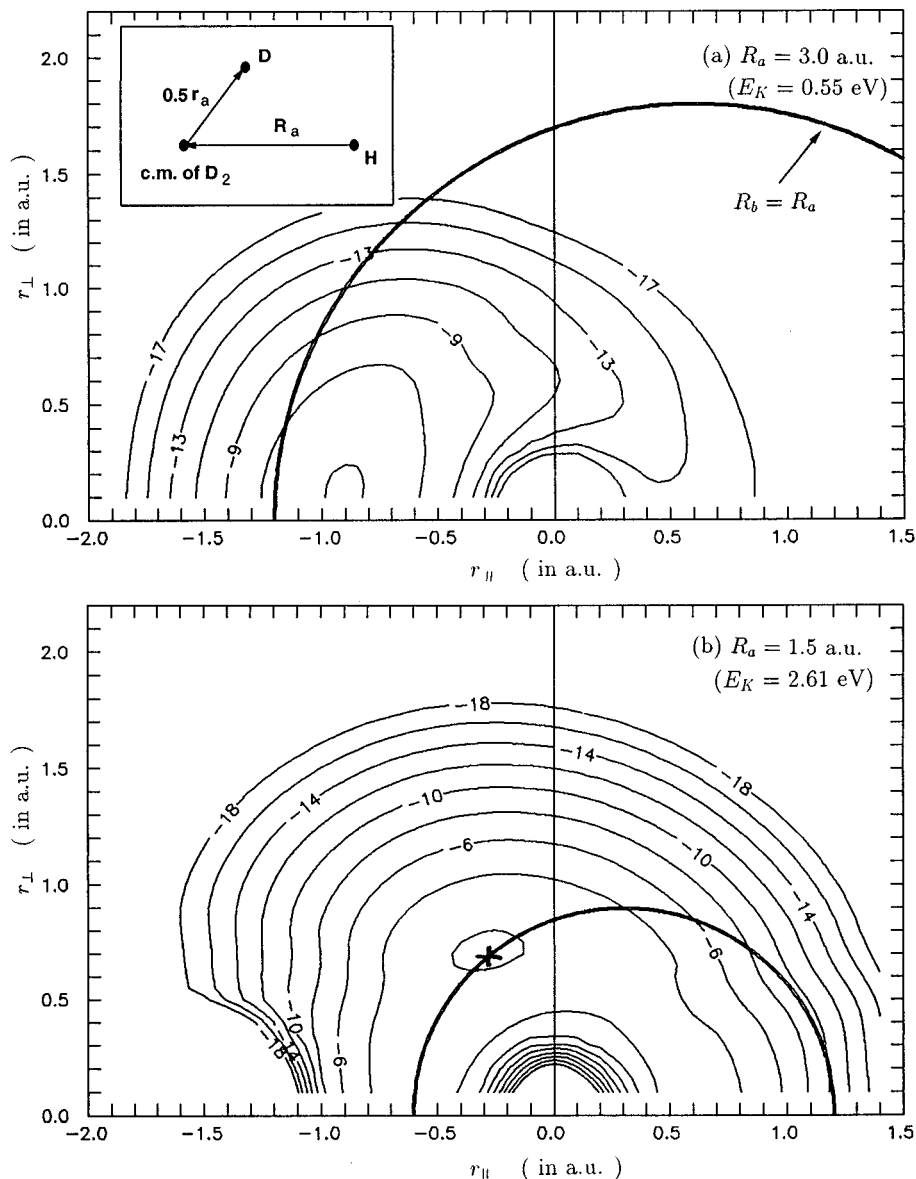


FIG. 4. Polar representations of contour maps of the kernel $|g(r_a, R_a, \hat{\mathbf{r}}_a, \hat{\mathbf{R}}_a)|$ for the reactive scattering $\text{H} + \text{D}_2(n_a=0, j_a=1) \rightarrow \text{HD}(n_b=0, j_b=0) + \text{D}$ at two different values of the reactant channel classical turning points (D_2 -H distance) $R_a=3.0$ and 1.5 a.u.

case, the dominance of the favored rotational polarization $m_a=0$ is not likely to occur. As an example, we consider the reaction $\text{He} + \text{H}_2^+(n_a=0, j_a=1) \rightarrow \text{HeH}^+(n_b=0, j_b=0) + \text{H}$ at low collision energies. Indeed, our computed ratio $\sigma(1)/\sigma(0)$ showed no marked preference of the $m_a=0$ rotational polarization, unlike the case of $\text{H} + \text{D}_2 \rightarrow \text{HD} + \text{D}$. We find from the present calculation of HD_2 that the angular structure of the distorted-wave function is noticeably anisotropic with a backward peak in the angular distribution of the projectile atom particularly at low collision energies, as shown in Fig. 3(a). This enhances a chance to form a collinear configuration with the target diatomic molecule in parallel with the incident H atom beam direction during reactive transition. Our computed kernel function showed the preference of a collinear configuration as shown in Fig. 4(a). Thus from this combined knowledge of the backward peaked

distorted-wave function and the collinear favored kernel function, we readily find that $m_a=0$ is the favored rotational polarization at low collision energies. Further, we discover that the favored collinear geometric configuration during the reactive transition lies in the direction of the incident beam. However, at sufficiently high collision energies, such collinearity disappears, reducing the relative strength of the $m_a=0$ rotational polarization. This is owing to the gradual reduction of the backward peak and the forward angle shift in the distorted-wave function. Thus thorough understanding of the favored rotational polarization is possible from the combinational examination of both the energy-independent kernel distribution function and the energy-dependent distorted-wave functions. If the attractive part of interaction is dominant, a backward peaked anisotropy in $\chi_a^{(+)}$ is not likely to occur, thus causing a relatively weak $m_a=0$ rota-

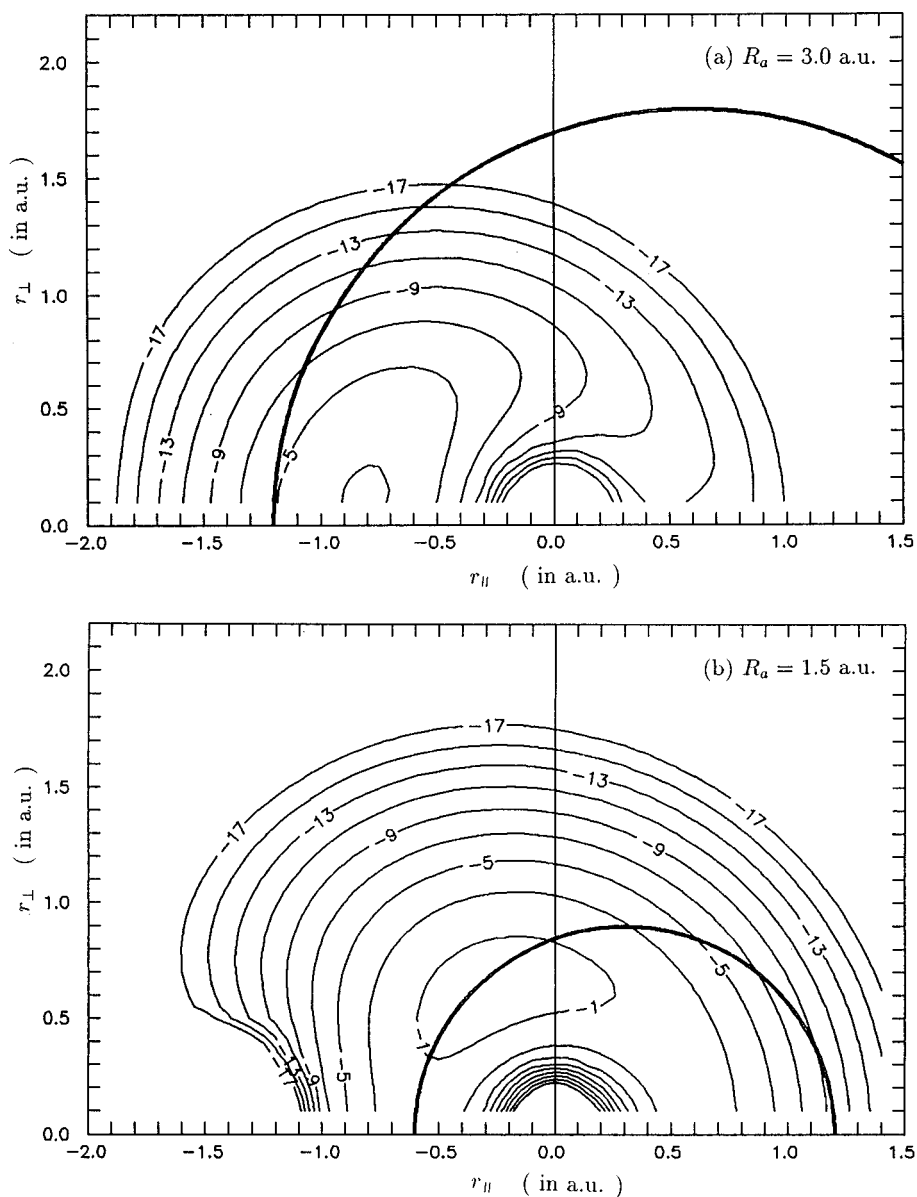


FIG. 5. Polar representations of contour maps of the pseudokernel $|\bar{g}(R_b, R_a, \hat{\mathbf{R}}_b \cdot \hat{\mathbf{R}}_a)|$ with the same reactive scattering as shown in Fig. 4.

tional polarization. Indeed, this is what we have found with the HeH_2^+ system, as discussed above.

In order to see whether the angular structures of the kernel distribution functions can be determined by the radial parts of the molecular wave functions alone, we now propose a “pseudokernel function” defined by

$$\bar{g}(R_b, R_a, \hat{\mathbf{R}}_a \cdot \hat{\mathbf{R}}_a) = \frac{u_{j_b}(r_b)u_{j_a}(r_a)}{r_b^{j_b+1}r_a^{j_a+1}}. \quad (4)$$

Here we ignore the dependence of the perturbation potential W in (2). Thus it is of great interest to see if there exists a significant alteration in the prediction of favored geometric configuration due to the ignorance of W . The pseudokernel distributions are displayed in Fig. 5 for comparison with the kernel distributions presented in Fig. 4. It is quite encouraging to find that the main feature of the angular structures of

the pseudokernel distributions is similar to that of the original kernel function. Thus the use of the pseudokernel has a merit of simplicity for investigating a favorite geometric configuration in elementary reaction processes before our involvement of complicated calculation of cross sections.

To the best of our knowledge, there exists no simple method of studying elementary state-to-state reactive scattering. We have explicitly demonstrated the usefulness of our approach for studying the energy dependence of rotational polarization by the combined examination of both the distorted-wave functions and the kernel distribution functions.

In summary, from the present simple approach we have found the following key features. (1) At low collision energies, the axis of the collinearly favored configuration aligns itself preferentially with the incident projectile beam direction during the moment of reactive transition; (2) as a consequence the preferential rotational polarization is $m_a=0$;

(3) at higher collision energies, it no longer remains the same, indicating the energy dependence of the rotational polarization; (4) rotational polarization arises from incoherence, that is, partial-wave interference does not affect rotational polarization; and finally (5) the pseudokernel function is found to be a highly useful map to easily study the intrinsic nature of favored geometry, thus avoiding complicated calculations.

For simplicity we have considered only the case of $j=1$ transferred angular momentum. Higher j angular momentum transfer will not alter the general feature of energy dependence found above, that is, rotational polarization of $m \neq 0$ becomes increasingly important at higher collision energies. This is owing to the forward angle shift of distorted-wave functions at any j value of angular momentum transfer at high collision energies, as previously discussed. In the present DWBA study, a dynamic contribution is introduced by allowing rearrangement, but not intermediate inelastic

scattering processes. However, as demonstrated in our earlier work [3], the structures of angular distributions are well reproduced, in agreement with the exact close-coupling calculation [4], as long as collision energies are not exceedingly high. Thus introduction of the inelastic scattering contributions is important for the absolute magnitudes of cross sections, but not for the relative magnitudes of angular distributions, thus validating the present study of rotational polarization.

We would like to stress that the present DWBA study has validity of reaction mechanism for qualitative understanding. For quantitative accuracy it is highly recommended to use nonperturbative methods [9–11].

This work was supported by the Center for Molecular Science at Korea Advanced Institute of Science and Technology and the Korean Ministry of Education BSRI program. The authors are grateful to Dr. Y. H. Jeon for helpful discussions.

-
- [1] S. H. Suck Salk, *Phys. Rev. A* **15**, 1893 (1977).
[2] S. H. Suck Salk and R. W. Emmons, *Phys. Rev. A* **24**, 129 (1981); S. H. Suck Salk, *Int. J. Quantum Chem.* **19**, 441 (1981).
[3] S. H. Suck Salk and C. K. Lutrus, *J. Chem. Phys.* **83**, 3965 (1985).
[4] G. C. Schatz, L. M. Hubbard, P. S. Dardi, and W. H. Miller, *J. Chem. Phys.* **81**, 231 (1984).
[5] J. N. L. Connor and W. J. E. Southhall, *Chem. Phys. Lett.* **108**, 529 (1984).
[6] S. H. Suck Salk, C. R. Klein, and C. K. Lutrus, *Chem. Phys. Lett.* **110**, 112 (1984).
[7] P. Halvick, M. Zhao, D. G. Truhlar, D. W. Schwenke, and D. J. Kouri, *J. Chem. Soc. Faraday Trans.* **86**, 1705 (1990).
[8] M. Nakamura, *J. Chem. Phys.* **95**, 4102 (1991).
[9] D. G. Truhlar and C. J. Horowitz, *J. Chem. Phys.* **68**, 2446 (1978); B. Liu, *ibid.* **58**, 1925 (1974); P. Siegbahn and B. Liu, *ibid.* **68**, 2457 (1978).
[10] (a) C. R. Klein and S. H. Suck Salk, *Chem. Phys. Lett.* **125**, 481 (1986); (b) S. H. Suck Salk and R. W. Emmons, *Phys. Rev. A* **29**, 2906 (1984); S. H. Suck Salk, *Phys. Rev. C* **43**, 812 (1991).
[11] G. C. Schatz and A. Kuppermann, *J. Chem. Phys.* **65**, 4642 (1976); A. Kuppermann and G. C. Schatz, *ibid.* **62**, 2502 (1975).